(Wark & Watson, 2000). Fujii et al. (1986) pointed out that in the Ol - Opx - basalt system, the connectivity of melt through grain edges was interrupted by Opx grains whose dihedral angle with melt is larger than 60 degree. Processes that control the fluid distribution in multi-phase rocks, however, are not fully understood. In this paper, we report preferential distribution of pore-fluid in the phase-boundaries (PBs), which is caused by the fact that migration of grain boundary of the same phases (GBs) dragging the fluid ceases at PB. We have synthesized wherlites with various forsterite (Fo) / diopside (Di) ratios with 1 - 1.5 wt percent water at 1.2 GPa and 1200 deg.C for 3 days and a week. Preference of aqueous fluid for one phase relative to the other, due to the differences in relative mineral-fluid interfacial energies, was not expected, because dihedral angles of Fo-fluid and of Di-fluid are similar at the experimental conditions. Most of the fluid was distributed in the GBs as pore fluids and no fluid inclusion was observed. We classified the pore fluids into two types, those surrounded by GBs (A-type) and by PBs (B-type). Regardless of Fo/Di ratios, proportion of B-type was larger in 1 week runs than in 3 days runs. The 80-90 percent of pore fluids were B-type in the 1 week runs. This result can be explained by the difference in mobility between GB and PB: namely, the pore fluids are dragged by the GBs much more rapidly than the PBs. During grain-growth of multi-phase rocks, pore fluids dragged by the GBs bump against the other mineral surface. This result leads to the implication that the connectivity of fluid in multi-phase rocks would be strongly affected by properties of the triple junctions composed of two different mineral phases and fluid, i.e., dihedral angle, faceting, and spatial distribution.

T42B MCC: Level 1 Thursday 1330h

The Tectonics of Tibet and East Asia Posters

Presiding: **A Meltzer,** Lehigh University; **A L Ault,** Lehigh University

T42B-0286 1330h POSTER

Tectonic Evolution of South China Coastal Provinces Since the Mid-Mesozoic

Lung Sang Chan[1] ((852) 2859-8002; chanls@hkucc.hku.hk); Manuel F Pubellier[2] (33144322273; pubellier@geologie.ens.fr); Phach V Phung[3] ((84-4) 834 5402; pvphach@vista.gov.vn); Medhi Mechti[2] (33144322273; mechti@geologie.ens.fr); Kar F Leung[1] (9289 2705; leungkarfai@graduate.hku.hk); Frederic Ego[2] (33144322273; ego@geologie.ens.fr)

[1]Hong Kong University, Pokfulam, Hong Kong 00000, Hong Kong

[2]Ecole Normale Superieure, 23 Rue Lhomond, Paris, 75 F-75231, France

[3]Hanoi Inst. Oceanography, Nghia Do - Cau Giay, Hanoi 208D, Viet Nam

Structural analysis using satellite imageries and detailed field studies with fault-slip data inversions in critical areas in Guangxi and Guangdong Provinces and Hong Kong reveal a polyphase tectonic history in the southeastern margin of South China, which essentially resulted from the passive reaction of the region to relative motions of neigboring plates during various times. Northward subduction of the Paleo Kula-Pacific plate under South China during Middle Jurassic-Early Cretaceous (Yenshanian arc) created a volcanic arc-back-arc setting with left-lateral shear partitioning along ductile fault zones and occasional left-lateral pull apart basins. Subduction was blocked in the late Upper Cretaceous resulting in shortening of the back-arc region and, reactivation of older faults (e.g . Nanxiong B. in Guangdong & Mirs B. in Hong Kong), followed by orogen collapse with local detachment faulting and narrow molasse basins. The extensional setting continued during Eocene-Oligogene with rifting characterized by the formation of offshore basins and expansion of the continental shelves. The extension was accompanied by left-lateral transtensional basins along NW-trending faults transfer faults (Baise B. in Guangxi), probably influenced by the left-lateral motion of the Red River Fault. The area entered a period of relative tectonic quiescence during early Oligocene-mid Miocene when South China Sea formed, with little stratigraphic record preserved on land. Tectonic exhumation in the Red River region at around 20 m.y. produced NW-trending extensional structures in the region. Southerly extrusion of the Kunming Block in the western part and subduction process in the east during the mid-Miocene-Pliocene resulted in E-W extension in the region, and local N-S compression in southern Tonkin. The westward subduction of the Philippine Plate and the reversal to right-lateral motion on the Red River Fault since 5 m.y.b.p. resulted in right-lateral motion and formation of pull-apart basins along NE-trending faults in the region (e.g. Haifeng B. in Guangdong). [Support from HKU and PROCORE programme is gratefully acknowledged].

T42B-0287 1330h POSTER

A Lower Paleozoic Plate Tectonic Model for the North Qilian Mountains, NW China

Houng-Yi Yang[1] (886-6-2757575 ext. 65421; hyyang@mail.ncku.edu.tw); Chien-Yuan Tseng[1] (yuan1515@yahoo.com.tw); Guo-Chao Zuo[2]; Han-Quan Wu[3]; Zhiqin Xu[4]; Jingsui Yang[4]

[1]Department of Earth Sciences, National Cheng Kung University, 1 Ta-Hsueh Road, Tainan 70101, Taiwan

[2]Gansu Bureau of Geology and Mineral Resources, 206 Houngxing Road, Lanzhou 730000, China

[3]Xi'an Institute of Geology and Mineral Resources, 166 Youyi Road, Xi'an 710054, China

[4]Institute of Geology, Chinese Academy of Geological Sciences, 26 Baiwanzhuang Road, Beijing 100037, China

Abstract The north Qilian mountains are a strongly-lineated Caledonian fold belt. Their mountain ranges, major rivers, fold axes, fault lines, and the spatial distribution of major rock types are all more or less parallel to one another and trend in NWW-SEE direction. The Caledonian plate tectonic structures have still been well preserved despite modifications by the Indosinian and Himalayan crustal disturbances. The north Qilian mountains may be considered as a plate suture zone which sutured the Alashan craton and the central-south Qilian craton in the lower Paleozoic time. This suture zone consists of an active continental margin, a passive continental margin, and an intervening oceanic domain. The southern margin of the Alashan craton was an active continental margin in the lower Paleozoic time, on which continental margin arcs, forearc basin, forearc ridge, and accretionary prism were very well developed. The northern margin of the central-south Qilian craton was chiefly a passive continental margin, but might be active locally in the lower Paleozoic time. The intervening oceanic domain consists of oceanic island arcs, oceanic islands, oceanic ridges, major oceanic floor, and backarc basin ocean floor. A Paleo-Qilian ocean with well-developed oceanic islands and oceanic ridges is presumed to have existed during the late Proterozoic-early Cambrian period. It started to contract in the mid-Cambrian and a Mariana type subduction occurred to have formed an oceanic island arc and a backarc basin. The Andean type subduction followed in the late-Cambrian through the Silurian periods, during which the paleo-Qilian oceanic lithosphere obliquely subducted northward beneath the southern margin of the Alashan craton, converting it from passive to active, and produced continental margin arc, forearc basin, forearc ridge, and accretionary prism, accompanied by the abundant granitoid intrusions. During the same period of time, the northern margin of the central-south Qilian craton had remained largely as a passive continental margin, but the paleo-Qilian oceanic lithosphere might have also subducted southward locally probably in the middle section of the north Qilian mountains. The cessation of the northerly oblique subduction in the late Silurian-Devonian period resulted an arc-continent collision and formed a backarc basin in the eastern section, and also left behind a segment of mid-oceanic ridge, an oceanic island arc, the enclosed remnant ocean, and a backarc basin on the surface of the earth in the western section. In summary, the lower Paleozoic plate tectonic structures of the north Qilian mountains are characterized by the orderly-arranged, well preserved mid-oceanic ridges, oceanic island arcs, accretionary prism, continental margin arcs, and backarc basins, and by the occurrence of Mariana-type and Andean-type subductions, dipolar subduction, and continental reworking and reactivation.

T42B-0288 1330h POSTER

Geochemical and Geochronologic Constraints on the Tectonic Evolution of Southeastern Tibet

Amanda L Booth[1] (650-725-0045; mbooth@pangea.stanford.edu); Peter K Zeitler[2] (peter.zeitler@lehigh.edu); William S.F. Kidd[3] (wkidd@atmos.albany.edu); Joseph L Wooden[4] (jwooden@usgs.gov); Bruce Idleman[2] (bdi2@lehigh.edu); Liu Yuping[5] (cdlyuping@cgs.gov.cn); C. Page Chamberlain[1] (chamb@pangea.stanford.edu)

[1]Stanford University, Dept. of Geological & Environ. Sci., Stanford, CA 94305

[2]Lehigh University, 31 Williams Dr, Bethlehem, PA 18015-3188

[3]31 Williams Dr, ES 315, Albany, NY 12222-0001

[4]U.S. Geol Survey, 345 Middlefield Road, Menlo Park, CA 94025

[5]Chengdu Institute of Mines and Geology, 82 Beisanduan, Chengdu 610082, China

The eastern syntaxis of the Himalayas is expressed in the crust as a rotation of topographic, structural, and lithologic features from dominantly east-west to approximately north-south trends. The axis of rotation of geologic features is coincidental with the high topography of the Namche Barwa region, the exposure of granulite-grade metamorphic rocks, and a major bend in the Tsangpo River. Within the Namche Barwa and subjacent terranes are numerous granitoids that are associated with various events contributing to the tectonic development of southeastern Tibet. Our combined geochronologic and geochemical investigation of these granitoids provides insight into mechanisms of granite formation and helps to constrain the distribution of terranes, timing of assembly, and magmatic processes operative in each. U-Pb SHRIMP ages establish a complex tectonic history for southeastern Tibet, with the presence of at least five magmatic episodes: ~250 Ma, ~120 Ma, 40-70 Ma, 18-25 Ma, and 3-10 Ma. Two lines of evidence suggest that the Namche Barwa massif is a product of local feedbacks between tectonic and surficial processes: 1) exceptionally young zircon ages (2.8–9.5 Ma) for samples collected from the Tsangpo river gorge correspond to a period of rapid denudation; 2) granitoid geochemistry within the massif core reveals high Rb/Sr ratios (>1.4), suggesting a fluid-absent (decompression) melting regime dominates near the core of Namche Barwa.

URL: http://www.ees.lehigh.edu/groups/corners/corners.html

T42B-0289 1330h POSTER

Tectonic Evolution of Mirs Bay Basin in Guangdong, South China

Kar Fai Leung[1] (852-9289-2705; leungkf1@graduate.hku.hk) ,

Lung S Chan[1] (852-2859-8002; chanls@hkucc.hku.hk)

Manuel Pubellier[2] (33-01-4432-2273; pubellie@geologie.ens.fr)

[1]Dept. of Earth Sciences, The University of Hong Kong, Pokfulam Road, Hong Kong 000, Hong Kong

[2]Laboratoire de Geologie, Ecole Normale Superieure-CNRS, 24 rue Lhomond, Paris 75231, France

Comprehensive structural analysis based on extensive field mapping and LANDSAT TM imageries indicates that several coastal basins in Guangdong Province of South China, including Mirs Bay, Daya Bay and Honghai Bay, are Late Cretaceous pull-apart basins structurally controlled by the NE-trending Linhuashan Fault Zone (LHFZ). A detailed study of Mirs Bay reveals a series of NW-trending high-angle normal faults dipping eastward on the southwestern margin of the basin and a broad NNW-striking fault zone on the eastern margin. The overall basin geometry is comparable to one at the mature stage of a classical pull-apart basin. The basin intersects the 500 m-wide NE-striking Tolo Channel Fault Zone, which displays a positive flower structure probably formed during the oblique subduction of the Paleo-Kula Plate under South China. Detailed study reveals a right-lateral motion postdating an earlier ductile deformation with a sinistral sense of motion along the fault zone. A southward facing thrust sheet exposed at the southern margin of the basin probably represents a detachment that formed during the collapse of the volcanic arc. Analysis of satellite images shows that the two basins located east of Mirs Bay are comparable to ones in the transitional stage of the pull-apart basin model. These three left-stepping basins are evidence for the predominantly strike-slip nature of the LHFZ during the subduction event, which has probably experienced several changes in the sense of motion during the Late Cretaceous through Tertiary in response to changes in the geodynamic setting of the surrounding blocks. (Support from HKU and PROCORE programme is gratefully acknowledged.)

T42B-0290 1330h POSTER

Rising the Himalayan-Tibetan plateau: A 3-D finite element model

Youqing Yang[1] (573-882-4449; yangyo@missouri.edu)

Mian Liu[1] (573-882-3784; lium@missouri.edu)

[1]University of Missouri, 101 Geology, Columbia, MO 65211, United States

More than 2000 km of the Earth's crust has been telescoped by the continuous Indo-Asian collision in the past 50-70 million years. Some models suggest that

1710 h **SM42E-05** Calibrating a Magnetotail Model for Storm/Substorm Forecasting: **W Horton**, S Siebert, M Mithaiwala, I Doxas

1725 h **SM42E-06** *INVITED* Vector and Scalar Field Visualization Techniques for Multispacecraft Space Physics Missions: **D A Roberts**, V Rezapkin, J Coleman, R Boller

1745 h **SM42E-07** Visualization and Data Analysis for CISM Models: **M Wiltberger**, T Guild, J G Lyon

---

T42A MCC: Level 1 Thursday 1330h
The Structure and Physical Properties of Grain Boundaries in Rocks III Posters *(joint with V)*

Presiding: **A Schubnel**, Lassonde Institute; **S Majumder**, University of Minnesota

1330 h **T42A-0265** *POSTER* Mechanical compaction of Bleurswiller sandstone : elastic wave velocities and permeability evolution: **J Fortin**, A Schubnel, Y Gueguen

1330 h **T42A-0266** *POSTER* Reduction of ionic diffusivity in nanopore water of geomaterials: **T Hirono**, S Nakashima, C J Spiers

1330 h **T42A-0267** *POSTER* An Experimental Study of Pressure Solution of Halite Under the Confocal Microscope: **Z Karcz**, E Aharonov, D M Ertas, R J Johnston, R S Polizzotti, C H Scholz

1330 h **T42A-0268** *POSTER* Mobility of Water Molecules on Brucite and Talc Surfaces by *Ab Initio* Potential Energy Surface and Molecular Dynamics Simulations: **H Sakuma**, T Tsuchiya, K Kawamura, K Otsuki

1330 h **T42A-0269** *POSTER* The Influence of Second Phases on Grain Boundaries of Mylonitic Microfabrics: Evidences From Natural Carbonate Mylonites: A Ebert, **M Herwegh**, A Pfiffner

1330 h **T42A-0270** *POSTER* A Close View Into the 3D Geometry of Grain-to-Grain Contacts and Surface Roughness in Sandstones Using Laser Scanning Confocal Microscopy: B Menendez, C David, **L Louis**, A Martinez Nistal

1330 h **T42A-0271** *POSTER* On Grain Boundary Wetting During Deformation: **S Majumder**, P H Leo, D L Kohlstedt

1330 h **T42A-0272** *POSTER* Connectivity of molten Fe alloy in mantle peridotite based on in situ electrical conductivity measurements: **T Yoshino**, M J Walter, T Katsura

1330 h **T42A-0273** *POSTER* Compositional effect on the dihedral angle between olivine and Fe-S liquid up to 20 GPa: Possibility of percolative core formation: **H Terasaki**, D C Rubie, D J Frost, F Langenhorst

1330 h **T42A-0274** *POSTER* The role of interfaces in plastic flow of two-phase rocks: X Xiao, G Dresen, **B Evans**

1330 h **T42A-0275** *POSTER* Melt-Grown Grain Textures of Eutectic Mixtures of Water Ice with Magnesium- and Sodium-Sulfate Hydrates and Sulfuric-Acid Hydrate Using Cryogenic SEM (CSEM): **C McCarthy**, S Kirby, W Durham, L Stern

1330 h **T42A-0276** *POSTER* Investigation Of The Transition To Nonlinear Acoustics In Driven Rods: **D Pasqualini**, T Jim, S Habib, K Heitmann, P Johnson

1330 h **T42A-0277** *POSTER* α-β Inversion in Quartz From Low Frequency Electrical Impedance Spectroscopy: **N Bagdassarov**

1330 h **T42A-0278** *POSTER* Damage and elastic recovery of calcite-rich rocks deformed in the cataclastic regime: **A Schubnel**, J Fortin, L Burlini, Y Gueguen

1330 h **T42A-0279** *POSTER* Modeling constitutive behavior and compaction localization for high porosity sandstone: **E R Grueschow**, J W Rudnicki

1330 h **T42A-0280** *POSTER* Rheological Behaviour and Microstructures of Natural Gypsum Experimentally Deformed in Simple Shear: **V Barberini**, L Burlini, E H Rutter, M Dapiaggi

1330 h **T42A-0281** *POSTER* Physical Properties of the Interface between a Mineral Inclusion and the Host Mineral: Monazite Inclusions in Fluorapatite: **D E Harlov**, R Wirth, H Foerster

1330 h **T42A-0282** *POSTER* The Impact of Olivine-Orthopyroxene Phase Boundaries on Mechanical Absorption: Inferences from Resonant Ultrasound Spectroscopy (RUS): J Lan, Y Wang, R S Lakes, **R F Cooper**

1330 h **T42A-0283** *POSTER* Anomalous Thermal Relaxation Induced by the Granular Composition of Berea Sandstone: **T Ulrich**, K R McCall, R Guyer

1330 h **T42A-0284** *POSTER* Microstructural Evolution and Grain Boundary Structure During Static Recrystallization in Synthetic Polycrystals of Sodium Chloride Containing Saturated Brine: J Urai, **O Schenk**

1330 h **T42A-0285** *POSTER* Grain-Scale Distribution of Aqueous Fluid in Wherlites: **T Ouchi**, M Nakamura

---

T42B MCC: Level 1 Thursday 1330h
The Tectonics of Tibet and East Asia Posters

Presiding: **A Meltzer**, Lehigh University; **A L Ault**, Lehigh University

1330 h **T42B-0286** *POSTER* Tectonic Evolution of South China Coastal Provinces Since the Mid-Mesozoic: **L Chan**, M F Pubellier, P V Phung, M Mechti, K F Leung, F Ego

1330 h **T42B-0287** *POSTER* A Lower Paleozoic Plate Tectonic Model for the North Qilian Mountains, NW China: **H Yang**, C Tseng, G Zuo, H Wu, Z Xu, J Yang

1330 h **T42B-0288** *POSTER* Geochemical and Geochronologic Constraints on the Tectonic Evolution of Southeastern Tibet: **A L Booth**, P K Zeitler, W S Kidd, J L Wooden, B Idleman, L Yuping, C P Chamberlain

1330 h **T42B-0289** *POSTER* Tectonic Evolution of Mirs Bay Basin in Guangdong, South China: **K Leung**, L S Chan, M Pubellier

1330 h **T42B-0290** *POSTER* Rising the Himalayan-Tibetan plateau: A 3-D finite element model: **Y Yang**, M Liu

1330 h **T42B-0291** *POSTER* Rapid Erosion at the Tsangpo Knickpoint and Exhumation of Southeastern Tibet: **M A Malloy**, P K Zeitler, B D Idleman, P W Reiners, L Zheng

1330 h **T42B-0292** *POSTER* The Eastern Syntaxis Seismic Experiment: **A Meltzer**, S Sol, B Zurek, Z Xuanyang, Z Jianlong, T Wenqing

1330 h **T42B-0293** *POSTER* Preliminary results of 10Be analyses from the eastern Himalayan syntaxis: evidence for unsteady erosion on two spatial scales.: **N J Finnegan**, B Hallet, J O Stone, D R Montgomery

1330 h **T42B-0294** *POSTER* Kinematic modeling of Neotectonic velocity field of the Persia-Tibet-Burma Orogen: **Z Liu**, P Bird

1330 h **T42B-0295** *POSTER* Source Mechanisms, Velocity Structures and Himalaya Tectonics: **F T Wu**, A F Sheehan, G Huang, G Monsalve

1330 h **T42B-0296** *POSTER* Mechanisms for creating accommodation space during early Tertiary sedimentation in Tibet.: **C Studnicki-Gizbert**, B C Burchfiel

1330 h **T42B-0297** *POSTER* Age of Initiation of the India-Asia Collision in the eastern Himalayas: **B Zhu**, W Kidd, D Rowley, B Currie

Eos, Transactions, American Geophysical Union AGU 2003 Fall Meeting Vol. 84, No. 46, 18 November 2003

AGU 2003 Fall Meeting

8-12 December 2003
San Francisco, California

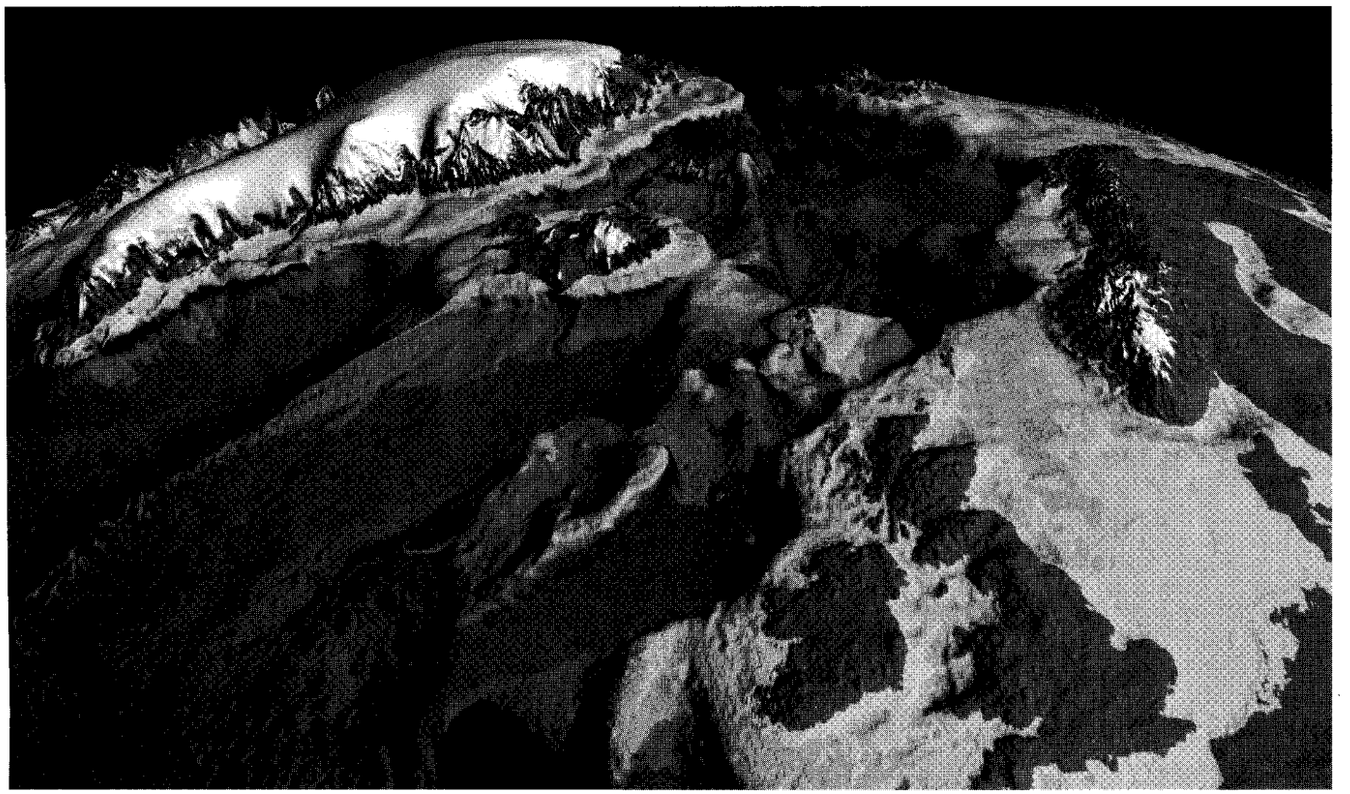

Published as a supplement to
Eos, Transactions, American Geophysical Union
Vol. 84, No. 46, 18 November 2003

AGU